initial absorbing state to the reactive state. Such rates could depend on the Franck-Condon factors between specific rotational-vibrational levels in the two states.

REFERENCES AND NOTES

1. K. S. Noll *et al.*, *Science* **267**, 1307 (1995).
2. R. A. West *et al.*, *ibid.*, p. 1296.
3. W. M. Jackson, P. S. Butterworth, D. Ballard, *Astrophys. J.* **304**, 515 (1986).
4. G. W. Cooper *et al.*, *Meteoritics* **30**, 500 (1995).
5. M. H. Thiemens and T. Jackson, *Lunar Planet. Sci. Conf.* **XXVI**, 1405 (1995).
6. C. E. Rees and H. G. Thode, *Geochim. Cosmochim. Acta* **41**, 1697 (1977).
7. R. Wieler *et al.*, *ibid.* **55**, 1709 (1991).
8. P. W. Bridgman, *Proc. Am. Acad. Arts Sci.* **74**, 399 (1941).
9. J. J. Colman and W. C. Trogler, *J. Am. Chem. Soc.* **117**, 11270 (1995).
10. K. Zahnle, M.-M. M. Low, K. Lodders, B. Fegley Jr., *Geophys. Res. Lett.* **22**, 1593 (1995).
11. Elemental analyses were performed by Desert Analytics: 26.72 weight % C and 72.70 weight % S ($CS_{1.02}$).
12. J. J. Colman and W. C. Trogler, preprint of paper presented at the 207th national meeting of the American Chemical Society, San Diego, CA, March 1994; ENV 67.
13. F. Z. Chen and C. Y. R. Wu, *Geophys. Res. Lett.* **22**, 2131 (1995).
14. J. I. Moses, M. Allen, G. R. Gladstone, *ibid.*, p. 1597.
15. E. Lellouch *et al.*, *Nature* **373**, 592 (1995).
16. M. Chin and D. D. Davis, *Global Biogeochem. Cycles* **7**, 321 (1993).
17. H. A. Weaver *et al.*, *Science* **267**, 1282 (1995).
18. J. Crovisier, D. Despois, D. Bockelée-Morvan, P. Colom, G. Paubert, *Icarus* **93**, 246 (1991).
19. This calculation assumes that the quantum yield for photodissociation equals 1, but this datum does not exist in the literature. Therefore, a direct measurement was undertaken. The quantum yield that we obtained for CS_2 removal at 193 nm, using an ArF eximer laser and N_2O photodissociation (quantum yield, 1.44; extinction coefficient, 8.95×10^{-20} cm^2) as an actinometer, was 0.5 to 1.
20. H. B. Niemann *et al.*, *Science* **272**, 846 (1996). A small signal was observed at 76 atomic mass units (amu), but no signal was observed at 78 amu. If solar abundances were obtained, there should have been an 8.02% abundance of the 78-amu isotopomer.
21. All $(CS_2)_x$ samples used for isotopic analysis were produced in a 2400-ml quartz Schlenk flask. About 1 to 2 ml of CS_2 was placed in the flask, which then was multiply (three times) freeze-pump-thaw degassed. Photochemical conversions were less than 5% for the isotopic measurements. Sample 1 was irradiated for 100 hours with a Pyrex-filtered 450-W, medium-pressure Hg lamp. The $(CS_2)_x$ was collected by suspension in acetone and centrifugation. Sample 2 was prepared by 2 weeks of solar irradiation (late July, 32°N latitude). We dislodged the $(CS_2)_x$ from the sides of the flask and collected it on weighing paper. Sample 3 was produced by 8 days of solar irradiation (early October). The polymer was solvent-collected, as for sample 1. The S isotopic composition of the $(CS_2)_x$ was determined by procedures described in (*22*).
22. X. Gao and M. H. Thiemens, *Geochim. Cosmochim. Acta* **57**, 3159 (1993). Isotopic compositions are reported in the conventional delta notation, in which
$$\delta^{34}S = \left[\frac{(^{34}S/^{32}S)_{\text{sample}}}{(^{34}S/^{32}S)_{\text{standard}}} - 1 \right] \times 1000$$
This quantifies the $^{34}S/^{32}S$ ratio in a sample, referenced to the standard S in CDT (Canyon Diablo triolite). Variations are reported in parts per thousand or per mil. The $\delta^{33}S$ ($^{33}S/^{32}S$) and $\delta^{36}S$ ($^{36}S/^{32}S$) ratios were also determined. Errors associated with $\delta^{33}S$ and $\delta^{34}S$ are ± 0.04 per mil and ± 0.15 per mil for $\delta^{36}S$. Figure 2 shows the isotopic results, normalized to the initial CS_2 isotopic composition ($\delta^{32}S = 4.24$, $\delta^{34}S = 8.25$, $\delta^{36}S = 15.26$ with respect to CDT).
23. M. H. Thiemens, in *Isotope Effects in Gas Phase Chemistry*, J. A. Kaye, Ed. (American Chemical Society, Washington, DC, 1992), pp. 138–153.
24. C. A. Goodrich, *Meteoritics* **27**, 327 (1992).
25. C. Lambert and G. H. Kimbell, *Can. J. Chem.* **51**, 2601 (1973).
26. L. E. Brus, *Chem. Phys. Lett.* **12**, 116 (1971).
27. A. Habib, R. Görgen, G. Brasen, R. Lange, W. Demtröder, *J. Chem. Phys.* **101**, 2752 (1994).
28. A. E. Douglas and E. R. V. Milton, *ibid.* **41**, 357 (1964).

29. We thank A. C. Kummel and E. Lanzendorf for use of the eximer laser. Supported by NSF (grant CHE-931940) and NASA (grants NAGW 3551 and NAGW 2251).

16 April 1996; accepted 10 June 1996

A Statistical Model of the Fluctuations in the Geomagnetic Field from Paleosecular Variation to Reversal

Pierre Camps* and Michel Prévot

The statistical characteristics of the local magnetic field of Earth during paleosecular variation, excursions, and reversals are described on the basis of a database that gathers the cleaned mean direction and average remanent intensity of 2741 lava flows that have erupted over the last 20 million years. A model consisting of a normally distributed axial dipole component plus an independent isotropic set of vectors with a Maxwellian distribution that simulates secular variation fits the range of geomagnetic fluctuations, in terms of both direction and intensity. This result suggests that the magnitude of secular variation vectors is independent of the magnitude of Earth's axial dipole moment and that the amplitude of secular variation is unchanged during reversals.

The way the geomagnetic field reverses itself remains poorly understood, because of the scarcity of reliable and sufficiently complete paleomagnetic records of the same reversal from widely distant sites at Earth's surface. Two main questions are still unanswered. First, are field reversals and excursions specific phenomena unrelated to paleosecular variation? Although excursions and reversals are sometimes considered as extrema of secular variation (*1*), all the statistical field models produced thus far by the paleomagnetic community are restricted to the description of paleosecular variation, which implies that the paleosecular regime (*2*) is physically distinct from the reversing regime. However, we know of no observation that has confirmed this view.

The second main question regards the composition (ideally, in terms of spherical harmonic coefficients) of the reversing field as compared with that of the so-called "stable" field. Absolute paleointensity data show unambiguously that the field strength is considerably reduced during reversals and excursions (*3*–*6*); therefore, a large reduction of the dipole moment is needed. Obviously, the axial dipole (AD) has to pass through zero as the field reverses. Our certainties stop here. The behavior of the equatorial dipole is not known, nor do we know whether the destiny of the nondipole terms is correlated with that of the dipole. Does the energy of the dipole transfer into that of some other terms (*7*), or does it reduce without any correlated change in the other terms (*8*)?

Paleomagnetic data allow an examination of these questions from a statistical standpoint, provided that the paleofield strength is taken into account. For this purpose, we compiled a paleomagnetic database from volcanic rocks that, in contrast to earlier databases (*9*, *10*), includes remanence intensity and covers the entire range of geomagnetic fluctuations, from paleosecular variation to reversal. The use of remanence intensity instead of paleofield strength was forced by the present scarceness of paleointensity data that precludes, in any region of Earth, a proper statistical description of paleofield strength. Assuming that the average remanence intensity is proportional to the average paleofield strength, we propose a statistical model of the local geomagnetic fluctuations. The agreement between our observations and the predictions of this model suggests that the magnitude of secular variation is not connected to the longer term variation of the AD moment.

Geomagnetic field fluctuations are generally analyzed after the local field vector is transformed into a virtual geomagnetic pole (VGP). Here, we use the local geographic reference frame because the VGP transformation becomes less physically significant

Laboratoire de Tectonique et Géophysique, Unité Associée au CNRS case 060, Université de Montpellier 2, Place Eugène Bataillon, 34095 Montpellier Cedex 5, France.

*To whom correspondence should be addressed.

as the field deviates more from its basically dipolar normal configuration. Consequently, our analysis will be carried out at a regional scale. The data consist of ~3000 cleaned remanence vectors obtained from basaltic lava flows less than 20 million years old. The data selection criteria and the basic assumptions legitimizing our approach are detailed and discussed in (11). Because of the poor geographic coverage of paleomagnetic data, only in three regions were the data subsets large enough to permit a statistical description of the field: Iceland (1915 vectors); a middle latitude region (30° to 60°, 437 vectors); and a low latitude region (0° to 30°, 389 vectors). The last two regions are rather wide, because they include data from sites with any longitude and belonging to both hemispheres.

No a priori hypothesis was made regarding the distribution of directions. For each region, the mean direction of the n unit vectors was calculated from an eigenvector analysis and the concentration parameter from its formulation, which may be used to describe any type of distribution, $\kappa = 1/(1 - R/n)$, where R is the resultant length (12). For the Icelandic data subset (Fig. 1), the distribution of directions clearly presents two main characteristics: It is rotationally symmetric, which is illustrated in Fig. 1A and was also formally tested (13), and it does not follow a Fisherian probability (Fig. 1B) (14). Although the formal tests are not as clear for the low and middle latitude regions as they are for Iceland, they do suggest that these two properties, including rotational symmetry, are valid at all latitudes, in contrast to the present-day situation in which the field vectors are not isotropic in the plane perpendicular to the mean field direction in the equatorial region (15). The rotational symmetry of local field directions agrees with the absence of VGP confinement, which was found with the use of another volcanic database (16). The third directional constraint is the concentration parameter κ, which decreases with latitude (11.0 for Iceland, 9.7 at middle latitudes, and 5.9 at low latitudes), as could be expected from the paleosecular variation analyses carried out in the VGP space (17).

In each of our three subsets, average remanence intensity decreases regularly as the direction deviates from the mean (Fig. 1C). Qualitatively similar observations have been reported, either in the VGP space (18) or in the local geographic space (5). In all cases, researchers have assumed that the remanence intensity of basaltic rocks was proportional to the paleofield strength. We make the same assumption (11). There are only two sites at Earth's surface for which rather numerous absolute paleointensity determinations have been carried out: Steens Mountain (4) and West Eifel (6). In both regions, a rapid decrease in field intensity is observed as the field deviates from the AD field direction, which is in qualitative agreement with the remanence data. The Icelandic data can be approximately fitted by two successive linear parts with different slopes and intersecting near 40° (Fig. 1C). This observation is also valid for the middle and low latitude regions. As a matter of convention, the domain in which the angular deviation from the mean direction is less than 40° will be called the "paleosecular field domain," and the "intermediate field domain" will then correspond to the complementary angular space. For the purpose of fitting our data with the model described below, we chose to characterize each plot of intensity versus angular deviation by s, the slope corresponding to the "paleosecular field domain" (0° to 40°). Our observations indicate that the local fluctuations of the geomagnetic field vector are characterized by a rotationally symmetric, non-Fisherian distribution that can be quantitatively specified for each region in terms of the parameters κ and s.

Our statistical model is meant to fit both the directional and the intensity data and to cover the entire range of geomagnetic fluctuations, from paleosecular variation (PSV) to reversals. The local field vector is the sum of two independent sets of vectors (Fig. 2). The first set consists of vectors directed along the average field direction and exhibiting a normal distribution of magnitude with a nonzero mean. The global analyses of the time-averaged paleomagnetic data obtained from volcanic rocks less than 5 million years old show that this direction corresponds, in terms of spherical harmonic analysis, to an AD coefficient plus a small (5%) axial quadrupole term, both reversing simultaneously (10, 19). For simplicity, this component will be called here the AD component. Its magnitude distribution can be written as $N(\mu_{AD}, \sigma^2_{AD})$, where N denotes a normal probability density function (pdf) whose mean is μ

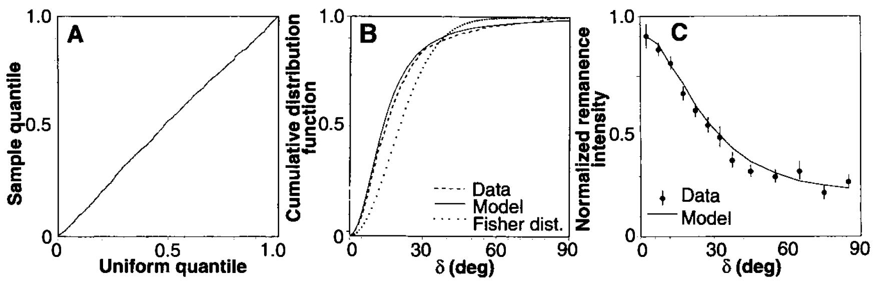

Fig. 1. Data and model for the Icelandic data set (0 to 16 million years ago, 1915 vectors). (**A**) Q–Q plot for the rotated declinations. The linearity observed between the sample quantile ($X_i = D'_i/2\pi$, where D'_i are the rotated declinations) and the quantile of the uniform distribution [$U_i = (i - 0.5)/n$, where n is the number of data] gives a graphical assessment of the plausibility of a circular symmetry of the local field directions about the principal axis [as we are dealing with both normal and reverse directions, we are concerned with the bipolar distribution; see (13), p. 164]. (**B**) Cumulative distribution function (cdf) for the angular distance (δ) measured from either the normal or the reverse end of the principal axis. The dashed curve is the empirical cdf calculated from the data. The solid curve indicates the model outcomes, assuming magnitude distributions N_{AD} (1, 0.2) and N_{SV} (0, 0.04). The dotted line is the theoretical cdf for a Fisherian distribution such that $\kappa_{Fisher} = \kappa_{data}$. (**C**) Geometric mean of the relative intensity versus δ. The vertical bars represent the standard errors. To calculate the slope s, which is used as a model constraint, we assumed a linear decrease in the intensity in the interval from 0° to 40°.

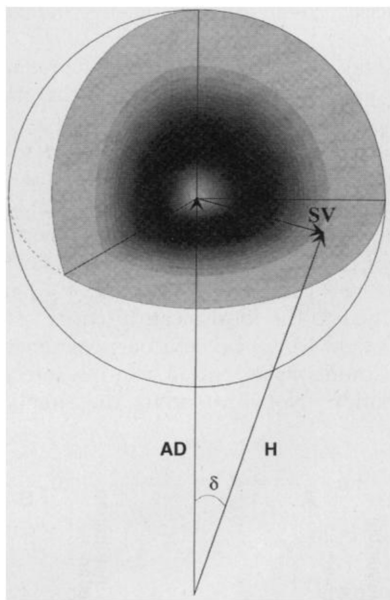

Fig. 2. Geometry of the local field vector (**H**); **H** is the sum of two independent sets of vectors: the secular variation (**SV**) vector set (uniform orientation, magnitude defined by a Maxwell-Boltzmann pdf) and the axial (**AD**) vector set (constant direction and magnitude defined by a nonzero mean Gaussian pdf). The Maxwell-Boltzmann pdf is represented here for a variance equal to 0.04. The **SV** vector lengths become more probable as the shaded sectors become more gray. The pdf of the axial vector intensity is not illustrated.

and whose standard deviation is σ.

The second set, which simulates an isotropic secular variation, consists of vectors having uniform orientation while their magnitude is distributed according to a Maxwell-Boltzmann pdf. This distribution, used by Cox (*15*) to simulate only the nondipole part of secular variation (SV), corresponds to that of the magnitude of a set of vectors with their Cartesian coordinates distributed as three independent random Gaussian variables having the same $N(0, \sigma^2_{SV})$ distribution (*20*). The vector sum of these two components is a rotationally symmetric non-Fisherian distribution (*21*).

The present model differs from PSV models that combine either dipole and nondipole fields (*15*) or equatorially symmetric and antisymmetric fields (*22*) but is similar in essence to the pioneering model of Irving and Ward (*23*). The physical basis of our model is the widely accepted idea that SV is created in the near-surface layers of the core by advection of the "basic dynamo field" produced by deep-seated fluid motions in the core (*24*). Hulot and Le Mouël (*25*) proposed that diffusion plays a major role in the building of the AD, which would therefore vary slowly. Independent of this variation, advection of the basic dynamo field near the core surface would be responsible for shorter time constant ("secular") variations, affecting in an isotropic way all the spherical harmonic coefficients including the AD.

Thus, only three parameters are required to specify the present model: the mean (μ_{AD}) and the variance (σ^2_{AD}) of the Gaussian pdf assumed for the slow variations of the axial field vector, plus one parameter (σ_{SV}) specifying the Maxwell-Boltzmann pdf assumed for SV. Furthermore, it is possible to limit the system to only two parameters (σ_{AD} and σ_{SV}) normalized to the local mean intensity of the AD field (μ_{AD}) because our experimental constraint yields only a relative intensity variation. Notwithstanding the simplicity of this model, the analytical expressions of κ and s as a function of the two model parameters are probably intractable. Hence, we used a Monte Carlo simulation (20,000 random combinations of each of the two vectors) to investigate its statistical characteristics. A simple case, assuming a constant AD field vector ($\sigma^2_{AD} = 0$), for which an analytic solution of κ as a function of σ^2_{SV} is available (*12*), was computed first to ensure that our simulation is operating correctly. Then, κ and s were calculated from the outcomes of computer simulations for several discrete values of σ^2_{AD} and σ^2_{SV}. Our model is not constrained when only one data parameter (κ or s) is known: various combinations of σ^2_{AD} and σ^2_{SV} could account for a particular value of κ or s. In contrast, combining κ and s should provide a single model if the directional and intensity data are both statistically representative of the local field fluctuations.

There is no doubt that our Icelandic data set (0 to 16 million years old) is the best documented and should be statistically representative. The model fits the paleomagnetic data remarkably well (Fig. 1): both the distribution of angular deviation and the dependence of the average field strength versus angular deviation are simulated almost exactly. For the low and middle latitude regions, there is only one parameter to adjust (σ_{SV}) because σ_{AD} is already known. Figure 3 shows the data and several fits obtained for the low latitude data set. For the corresponding time interval (0 to 5 million years ago) σ^2_{AD} was found to be 0.25 from the Icelandic data set. The model cannot simultaneously fit the two plots displayed (Fig. 3): depending on the diagram used, σ^2_{SV} varies from 0.17 to 0.44. We believe that this uncertainty is due to the poor representativeness of the data, as is attested by the irregularity of the cumulative plot of frequency versus angular deviation (Fig. 3B), which throws some doubt on the actual value of κ. One can also have some doubts about the statistical representativeness of the intensity diagram (Fig. 3C) because of the very small number of distinct excursions or reversals recorded in the low latitude data set. We therefore suggest provisionally that to model the field at this latitude a value of $\sigma^2_{SV} = 0.30 \pm 0.15$ be used. A similar approach applied to the middle-latitude data (0 to 16 million years ago) yields a more constrained σ^2_{SV} value (0.40 ± 0.05).

As a further test of the validity of our model, we have calculated the distribution of relative virtual dipole moments (VDMs) deduced from our Icelandic local model. Figure 4 compares this distribution to the observed one, obtained from a compilation of Thellier-type paleointensity data carried out from nonintermediate directions obtained from all over the world (*26*). There is no obvious disagreement between our model and the experimental data, which suggests that the model correctly predicts the paleofield strength distribution.

Four main sets of conclusions can be drawn from this study.

1) The fact that paleomagnetic directions, although axisymmetrically distributed, do not obey a Fisherian distribution, has a fundamental geomagnetic significance: The field fluctuations are not isotropic. They are much larger along the AD direction. Our model suggests that the variability of the AD results mainly from the slow changes due to diffusion (*25*), which are not considered in SV analyses.

2) We used intensity of remanence as a substitute to paleofield strength because paleointensity data are at present too scarce to provide a statistically valid description of the field fluctuations in magnitude. It is clear, however, that the validity of the

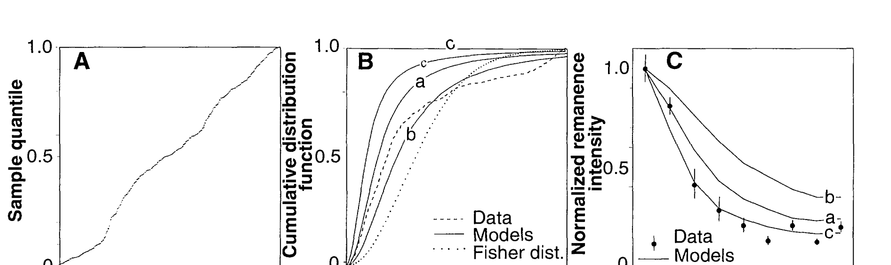

Fig. 3. (**A** through **C**) Data and models for the low latitude sites (latitude 0° to 30°, 0 to 5 million years ago, 389 vectors). Same diagrams as in Fig. 1. The variance of the AD vector, calculated from the Icelandic data set (0 to 5 million years ago), is 0.25 for the three different models represented by a, b, and c in (B) and (C). Then we fixed σ^2_{SV} assuming either that $\sigma^2_{SV}/\sigma^2_{AD}$ is independent of latitude (model a), $\kappa_{model} = \kappa_{data}$ (model b, with $\sigma^2_{SV} = 0.44$) or $s_{model} = s_{data}$ (model c, with $\sigma^2_{SV} = 0.17$).

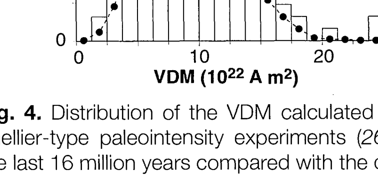

Fig. 4. Distribution of the VDM calculated from Thellier-type paleointensity experiments (*26*) for the last 16 million years compared with the distribution simulated from the Icelandic model. VDMs associated with transitional VGPs (VGP latitude < 40°) are not included. The distribution of paleointensity (which is not considered for specifying the model parameters) seems therefore to be correctly simulated by this model.

present field model needs to be confirmed by absolute paleointensity measurements.

3) Even through the use of remanence intensity, paleomagnetic data remain too scarce to allow the elaboration of a reliable global field model. It is necessary to establish first the geographic dependence (on both latitude and longitude) of the amplitude of SV as expressed by σ^2_{SV}.

4) The fundamental assumption in our model is the independence of the magnitude of SV vectors regardless of the longer term variation of the AD even when it decreases to zero. The agreement between our model and the paleomagnetic data presently available suggests that this hypothesis is verified. This conclusion supports the tangential geostrophic model of SV, which, according to theoretical inferences (*27*), implies the independence of the magnitude of SV vectors with respect to the magnitude of the AD. No transfer of the AD energy into other harmonic coefficients seems to occur during reversal, contrary to hypotheses proposed in several reversal models (*7*). We have no evidence for the decrease in the magnitude of SV vectors during reversal that can be inferred from the results of a recent computer simulation of an individual geomagnetic reversal (*28*).

REFERENCES AND NOTES

1. D. Gubbins, *Rev. Geophys.* **32**, 61 (1994); C. G. A. Harrison, *J. Geomagn. Geoelectr.* **47**, 131 (1995).
2. In the literature, no clear physical distinction is made between secular and paleosecular variation processes. According to the model presented in this report, the paleosecular variation is the sum of SV and a slower variation of the AD.
3. R. S. Coe, S. Grommé, E. A. Mankinen, *J. Geophys. Res.* **89**, 1059 (1984); M. Marshall, A. Chauvin, N. Bonhommet, *ibid.* **93**, 11681 (1988); P. Roperch, N. Bonhommet, S. Levi, *Earth Planet. Sci. Lett.* **88**, 209 (1988); S. Levi *et al.*, *ibid.* **96**, 443 (1990).
4. M. Prévot, E. A. Mankinen, R. S. Coe, C. S. Grommé, *J. Geophys. Res.* **90**, 10417 (1985).
5. A. Chauvin, P. Roperch, R. A. Duncan, *ibid.* **95**, 2727 (1990).
6. E. Schnepp, *Geophys. J. Int.* **116**, 688 (1994).
7. K. A. Hoffman, *Science* **196**, 1329 (1977); I. Williams and M. Fuller, *J. Geophys. Res.* **86**, 11657 (1981); D. Gubbins and R. S. Coe, *Nature* **362**, 51 (1993).
8. C. Constable, *J. Geophys. Res.* **95**, 4587 (1990); C. Mary and V. Courtillot, *ibid.* **98**, 22461 (1993).
9. S. Lee, thesis, Australian National University, Canberra (1983).
10. X. Quidelleur, J. P. Valet, V. Courtillot, G. Hulot, *Geophys. Res. Lett.* **21**, 1639 (1994); C. L. Johnson and C. G. Constable, *Philos. Trans. R. Soc. London Ser. A* **354**, 89 (1996).
11. For each flow, we calculated the average direction and remanence intensity after alternating field-cleaning at 10 mT or more. The proportionality between this remanence and the paleofield intensity holds if (i) the primary remanence is a thermoremanent magnetization, which is believed to be the case for basaltic rocks; (ii) secondary magnetizations are absent or were destroyed by the cleaning treatment; and (iii) the effects of mineralogical variations (from one flow to the other) on remanence intensity are averaged out. For the best documented region (Iceland), we demonstrate (in P. Camps and M. Prévot, in preparation) that the viscous secondary remanence left after treatment is negligible. The effects of mineralogical variations are almost entirely averaged out (Figs. 1C and 3C), as attested by the small dispersion of data (all calculated from distinct classes). The database is available through anonymous FTP at ftp.dstu.univ-montp2.fr; use your e-mail address as the password and type cd pub/paleomag.
12. A. Cox, *Geophys. J. R. Astron. Soc.* **8**, 345 (1964). This is the best estimate for κ (which is an inverse measure of the sample dispersion) when the distribution is non-Fisherian.
13. We used the test statistic P_n, as described in *Statistical Analysis of Spherical Data*, N. I. Fisher, T. Lewis, B. J. J. Embleton, Eds. (Cambridge Univ. Press, Cambridge, 1987), p. 165.
14. The formal testing procedures are given in (*13*), p. 122; see also M. A. Stephens, *J. Am. Stat. Assoc.* **69**, 730 (1974). All formal tests (Kolmogorov, Cramer, Kuiper, Watson) strongly reject the Fisher distribution hypothesis (at 99% confidence).
15. A. Cox, *Geophys. J. R. Astron. Soc.* **20**, 253 (1970).
16. M. Prévot and P. Camps, *Nature* **366**, 53 (1993).
17. P. L. McFadden and M. W. McElhinny, *Geophys. J. R. Astron. Soc.* **78**, 809 (1984).
18. R. L. Wilson, P. Dagley, A. G. McCormack, *ibid.* **28**, 213 (1972); L. Kristjansson and I. McDougall, *ibid.* **68**, 273 (1982); J. L. Lin, K. L. Verosub, A. P. Roberts, *Geophys. Res. Lett.* **21**, 525 (1994).
19. R. T. Merrill and M. W. McElhinny, *Rev. Geophys. Space Phys.* **15**, 309 (1977).
20. K. Hirano, in *Encyclopedia of Statistical Sciences*, Kotz *et al.*, Eds. (Wiley, New York, 1982), vol. 7, pp. 647–649.
21. This distribution becomes Fisherian only if $\sigma_{AD} = 0$. See, for example, K. V. Mardia, in *Statistics of Directional Data*, (Academic Press, London, 1972), pp. 232–233. The shape of the observed distribution of directions could be fitted by a Bingham distribution.
22. P. L. McFadden, R. T. Merril, M. W. McElhinny, *J. Geophys. Res.* **93**, 11583 (1988).
23. E. Irving and M. A. Ward, *Pure Appl. Geophys.* **57**, 47 (1964).
24. D. Gubbins, *J. Geophys. Res.* **93**, 3413 (1988).
25. G. Hulot and J. L. Le Mouël, *Phys. Earth Planet. Inter.* **82**, 167 (1994).
26. M. Prévot, M. E. M. Derder, M. McWilliams, J. Thompson, *Earth Planet. Sci. Lett.* **97**, 129 (1990).
27. J. L. Le Mouël, *Nature* **311**, 734 (1984).
28. G. A. Glatzmaier and P. H. Roberts, *ibid.* **377**, 203 (1995).

29. We thank D. K. Bingham, S. C. Bogue, E. Mankinen, P. Roperch, and H. Shibuya for providing unpublished paleomagnetic data and R. Coe for reviewing the first version of this manuscript. This research was completed while P.C. held the position of postdoctoral researcher at the University of California, Santa Cruz, supported by a Ministère de l'Enseignement Supérieur et de la Recherche grant. Contribution CNRS-INSU-DBT "Terre Profonde" 55.

12 March 1996; accepted 13 June 1996

Absorption of Solar Energy in the Atmosphere: Discrepancy Between Model and Observations

Albert Arking

An atmospheric general circulation model, which assimilates data from daily observations of temperature, humidity, wind, and sea-level air pressure, was compared with a set of observations that combines satellite and ground-based measurements of solar flux. The comparison reveals that the model underestimates by 25 to 30 watts per square meter the amount of solar energy absorbed by Earth's atmosphere. Contrary to some recent reports, clouds have little or no overall effect on atmospheric absorption, a consistent feature of both the observations and the model. Of several variables considered, water vapor appears to be the dominant influence on atmospheric absorption.

Recent studies indicate that there are substantial discrepancies between models and observations in the disposition of solar energy within Earth's climate system (*1–6*). Of the global average solar energy incident at the top of the atmosphere (TOA) (342 W m^{-2}), approximately 30% (102 W m^{-2}) is reflected back to space; the remainder (240 W m^{-2}) is absorbed by the atmosphere and the surface. The partitioning of this absorbed energy between the atmosphere and the surface is an important factor in determining the circulation of the atmosphere and the resulting temperature distribution (*7*), and is now the subject of debate.

Comparison of a general circulation model (GCM) with observations at 720 surface sites collected in the Global Energy Balance Archive (GEBA) (*8*) showed that the model overestimates by 10 to 15 W m^{-2} the global average solar flux absorbed by the surface (*1*). This result is consistent with an excess of 9 to 18 W m^{-2} in the downward solar irradiance at the surface in four other models, which were compared with observations at 93 GEBA sites (*2*).

The global mean solar flux absorbed in the atmosphere in four GCMs ranges from 56 to 68 W m^{-2} (*3*). These values are considerably smaller than those derived from observations at ~1000 GEBA sites and extended globally by means of empirical relations, 98 W m^{-2} (*8*), and are closer to the atmospheric absorption value derived from satellite-based estimates of surface flux, 65 to 83 W m^{-2} (*3*). The satellite-based estimates use radiative transfer codes to determine atmospheric absorption, so that comparing GCM absorption with satellite-based absorption is essentially a comparison of models. However, the upper end

Department of Earth and Planetary Sciences, Johns Hopkins University, Baltimore, MD 21218, USA. E-mail: arking@aa.gsfc.nasa.gov